Progress Report on NASA Grant NAG5-1609

Venus in Motion

An Animated Video Catalog of Pioneer Venus Orbiter Cloud Photopolarimeter Images

P-15

for the period
June 15, 1991 - December 31, 1991

Sanjay S. Limaye
Principal Investigator

Space Science and Engineering Center
University of Wisconsin-Madison
1225 West Dayton Street
Madison, Wisconsin 53706

(608)262-0544
E-Mail: Limaye@macc.wisc.edu

SUMMARY

Images of Venus acquired by the Pioneer Venus Orbiter Cloud Photopolarimeter during the 1982 opportunity have been utilized to create a short video summary of the data. The raw roll by roll images were first navigated using the spacecraft attitude and orbit information along with the CPP instrument pointing information. The limb darkening introduced by the variation of solar illumination geometry and the viewing angle was then modelled and removed. The images were then projected to simulate a view obtained from a fixed perspective with the observer at 10 Venus radii away and located above a Venus latitude of 30^{O} south and a longitude 60^{O}W. A total of 156 images from the 1982 opportunity have been animated at different dwell rates.

INTRODUCTION

Images acquired from the Pioneer Venus Orbiter Cloud Photopolarimeter (OCPP) since 1978 have provided useful information about the temporal variation of the appearance of Venus in solar reflected ultraviolet light and allowed a monitoring of the cloud motions over an extended period (Rossow et al. 1991; Limaye et al., 1988; Del Genio and Rossow, 1982). As the orbit of the Pioneer Orbiter spacecraft is nearly fixed in space and since the imaging data can normally be acquired only during the apoapsis function of the orbit, the period during which the images can be obtained in each orbit of Venus around the sun is typically only about three months, although occasional opportunities to image exist at other times. The results of the Pioneer Venus mission have been extensively summarized in **Venus** (Hunten et al., Eds). The CPP instrument is described in detail by Russel et al. (1977), and early results obtained therefrom have been presented by Travis et al. (1979a, 1979b); Kawabata et al. (1980); Rossow et al. (1980).

The Images

OCPP acquires images of Venus by the spin scan technique. Unlike the vidicon camera images obtained of Venus previously by Mariner 10 spacecraft (Murray et al., 1974), the OCPP images are created a scan at a time as the spacecraft spin sweeps the CPP field-of-view across the disk of Venus in the east-west direction. The movement of the orbiter spacecraft in its 24-hr 105^{o} inclination orbit (with an eccentricity of 0.84 and a peri-apsis of typically 150 km) allows the mapping by nearly contiguous scans in the north-south direction. As a result, the raw roll-by-roll images of Venus exhibit considerable geometric distortion, and for quantitative or qualitative examination of the images a remapping of the data is performed. Figure 1 shows 4 images in the raw roll-by roll format acquired an orbits 1179/1180 (Image #s 889-892) acquired on month, 27 February 1982. Figure 2 shows their rendition into a latitude-longitude map with a resolution of 0.25^{o}. Figure 3 shows the same images but in a perspective view from a vantage point at 30^{o}S and 60^{o}W at a distance of 10 R_V. In the mapping process (Figures 2 and 3) the shading due to changing geometry has also been accounted for as described below.

The time taken to acquire one image of Venus is typically 4 hours, such that typically 4 complete images can be acquired per 24-hr orbit. Due to the high eccentricity of the orbit however the images acquired just after periapsis require only about 2.5 hr whereas the ones at apoapsis can take as much as 5 hours. During this time the clouds rotate from east to west at

speeds ranging from 70 to 100 ms^{-1} in mid-latitudes. Thus along with the solar illumination geometry the appearance of Venus changes somewhat during the acquisition of a given image. Both of these effects can be accounted for to create a pseudo snapshot of Venus that mimics the appearance of Venus such that the illumination geometry is the same for each point (image normalization) and the relative distances between the cloud features are accurate at a given time. This process requires not only the knowledge of the winds or the cloud motions but also the instantaneous position of the sun relative to Venus during the course of the image. Fortunately the cloud motions have an imperceptible effect on the appearance and in the video catalog this movement has been ignored. Similarly the relative motion of the sun during the four hour period also has an insignificant effect for most analysis, but can be taken account of explicitly in the image navigation process, i.e. the task of relating each image co-ordinate to the Venus fixed co-ordinates.

Limb Darkening Removal

Previous work (Limaye, 1984) has shown that for most purposes the limb darkening can be reasonably well modelled by the Minnaert Law:

$$I\mu = I_0 (\mu\mu_0)^{\beta}$$

where μ and μ_0 represent the cosines of the viewing and the solar zenith angles, I_0, a constant can be thought of as the normal albedo, and β is an exponent such that $0 < \beta < 1$. I_0 and β can be readily obtained either by a linear least squares regression or by a robust technique from the calibrated intensity data (i.e. by removing the dark noise level of 15 dn from the raw data). If the Minnaert Law was obeyed perfectly then the features can be described by the observed deviations from an auxiliary intensity of the lit planet described only by I_0, μ and μ_0. That this is not so is illustrated by the actual values of the Minnaert slope and intercepts determined from each image as shown in Figure 4a and 4b. The quality of the regression fits is indicated by the linear correlation coefficient between $\log(I\mu)$ and $\log(\mu\mu_0)$ and is shown in Figure 4c. A short term periodicity is seen in each of these figures that indicates a dependence on the phase angle of Venus relative to the Pioneer Venus orbiter. As the phase angle varies systematically for each of the four images per orbit acquired during 1982, the Minnaert slope and intercepts show systematic variation. The coefficients determined for each image shown in the animation are given in Appendix I.

Figures

Figure 1. A series of four consecutive images (#s 889-892) acquired on orbits 1179/1180 (February 27, 1982) in the original, roll-by-roll format. The breaks in the images are when the roll-index pulse is shifted to accommodate the disk of Venus in the 1016 byte buffer of the CPP as it sweeps across the disk of Venus. During the periapsis portion of the orbit when the Pioneer orbiter spacecraft is closer to Venus, the apparent size of Venus exceeds the angular sweep triggered by the roll index pulse as the spacecraft moves in its orbit requiring changing the offset when the data acquisition begins. These shifts are detected from the instrument housekeeping data and used for navigating the data. The shape distortions are caused by the drift of the spacecraft sub-point longitude and changing range to Venus as the orbiter moves in its inclined, elliptical orbit. South is up and east is to the right in these images such that the view of Venus is upside down and backwards in the raw format. This is taken care of in the mapping process. The image center time, orbit number, phase angle and the location of the sub-spacecraft and sub-solar points when the CPP optic axis is directed at Venus center (i.e., the center time) is noted on each image.

Figure 2. A rectilinear representation of the images shown in Figure 1. The scale is 0.25^{o} in latitude and longitude. The images have been brightness normalized using the Minnaert Law coefficients determined for each image as described in the text.

Figure 3. A perspective view of the same images (Figure 1) from a vantage point above 30^{o}S and 60^{o}W longitude at a distance of $10R_{V}$.

Figure 4. Minnaert slope (a) and intercept found by least squares regression for each image. The regression coefficient is shown in c. A regular phase dependence of all three is apparent. The short term variations as seen on every orbit are also due to changes in the phase angle as the subspacecraft point varies from image to image due to the inclined elliptic orbit of the Pioneer Venus Orbiter.

REFERENCES and BIBLIOGRAPHY

Del Genio, A.D., and W.B. Rossow, 1982: Temporal variability of ultraviolet cloud features in the Venus atmosphere. *Icarus*, **51**, 391-415.

Hunten, D.M., L. Colin, T.M. Donahue, and V.I. Moroz, Eds., 1983: **Venus**, University of Arizona Press, 1143 pp.

Kawabata, K., D.L. Coffeen, J.E. Hansen, W.A. Lane, M. Sato, and L.D. Travis,1980: Cloud and haze properties from Pioneer Venus polarimetry. *J. Geophys. Res.*, **85**, 8129-8140.

Limaye, S.S., 1988: Venus atmospheric circulation: known and unknown. *Adv. Space Res.*, **10**, 91-101.

Limaye, S.S., C. Grassotti, and M.J. Kuetemeyer, 1988: Venus: Cloud level circulation during 1982 as determined from Pioneer Cloud Photopolarimeter images. I. Time and zonally averaged circulation. *Icarus*, **73**, 193-211.

Limaye, S.S., 1988: Venus: Cloud level circulation during 1982 as determined from Pioneer Cloud Photopolarimeter images. II. Solar longitude dependent circulation. *Icarus*, **73**, 212-226.

Limaye, S.S., 1987: Atmospheric Dynamics on Venus and Mars. *Adv. Space Res*, Planetary Studies, Eds. G.M. Keating, R.W. Shorthill, H. Masursky, and L.S. Elson, Vol 7, No. 12, 39-53.

Limaye, S.S., C. Grassotti, and M.J. Kuetemeyer, 1986: Cloud level circulation during 1982: Pioneer Venus manual tracking results. *Bull. Amer. Astron. Soc.* **18**, 824.

Limaye, S.S., 1984: Morphology and movements of polarization Features on Venus, *Icarus*, **57**, 362-385.

Rossow, W.B., A.D. Del Genio, S.S. Limaye, and L.D. Travis, 1980: Cloud morphology and motions from Pioneer Venus images. *J. Geophys. Res.*, **85**, 8107-8128.

Rossow, W.B., A.D. Del Genio, and T. Eichler, 1990: Cloud-tracked winds from Pioneer Venus OCPP images. *J. Atmos. Sci.* **47**, 2053-2084.

Russel, E., L. Watts, S. Pellicori, and D. Coffeen, 1977: Orbiter Cloud Photopolarimeter for the Pioneer Venus mission. *Proc. Soc. Photo Opt. Instrum. Eng.*, **112**, 28-44.

Travis, L.D., D.L. Coffeen, A.D. Del Genio, J.E. Hansen, K. Kawabata, A. A. Lacis, W.A. Lane, S.S. Limaye, W.B. Rossow, and P.H. Stone, 1979a: Cloud images from the Pioneer Venus Orbiter, *Science*, **205**, 74-76.

Travis, L.D., D.L. Coffeen, J.E. Hansen, K. Kawabata, A.A. Lacis, W.A. Lane, S.S. Limaye, and P.H. Stone, 1979b: Orbiter Cloud Photopolarimeter investigation, *Science*, **203**, 781-784.

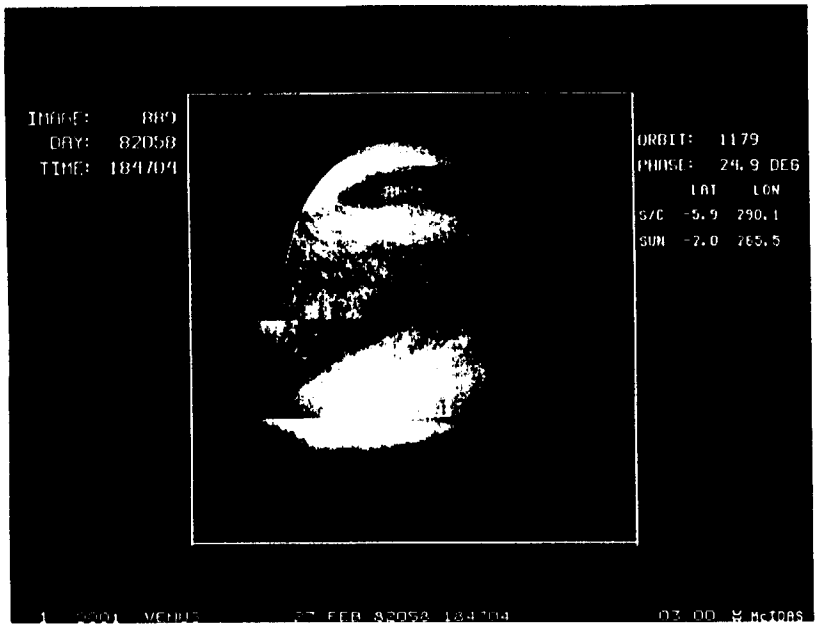

Figure 1a.

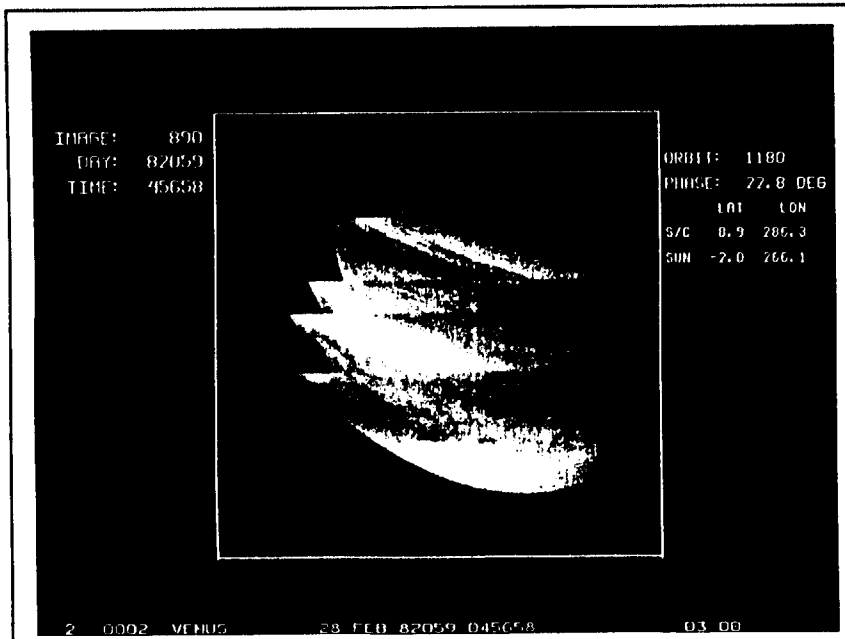

Figure 1b.

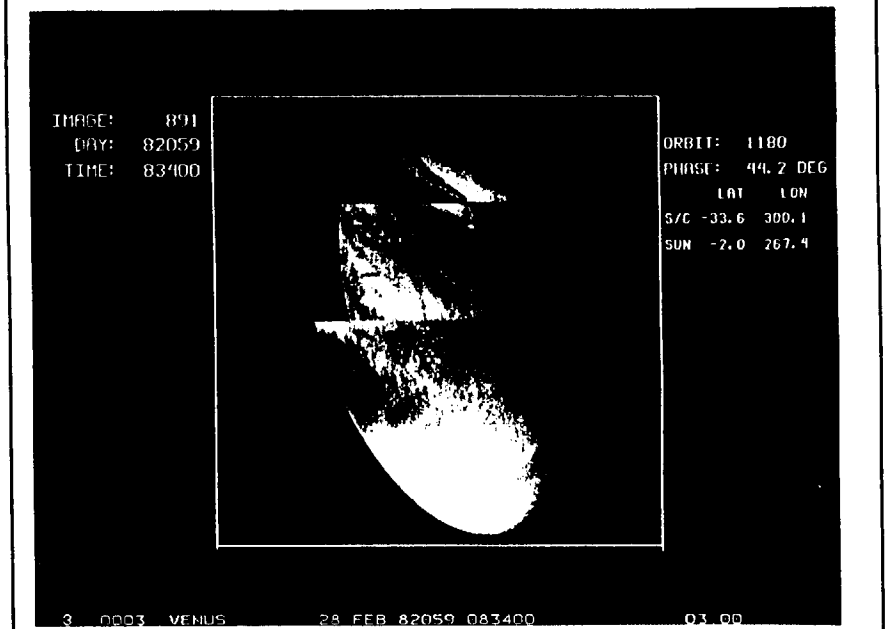

Figure 1c.

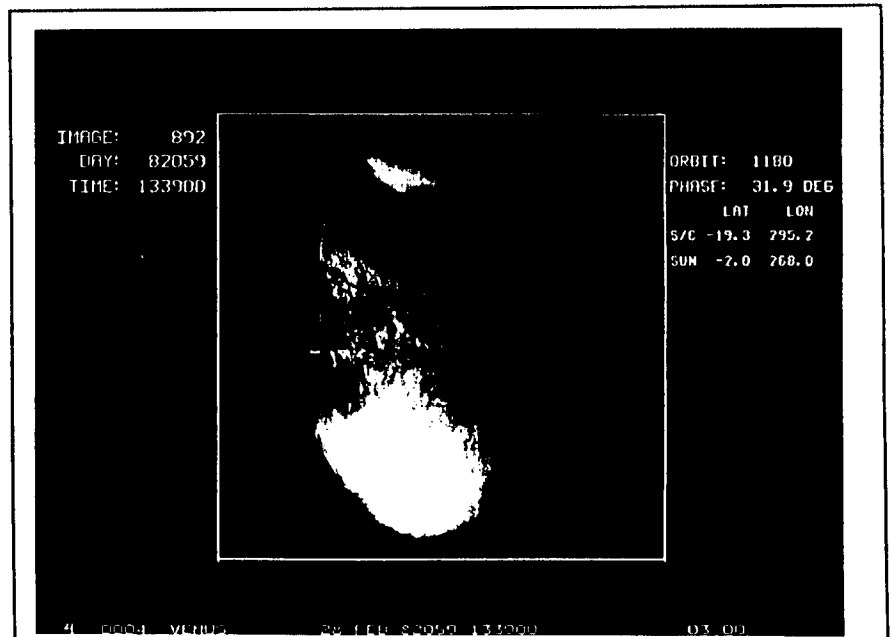

Figure 1d.

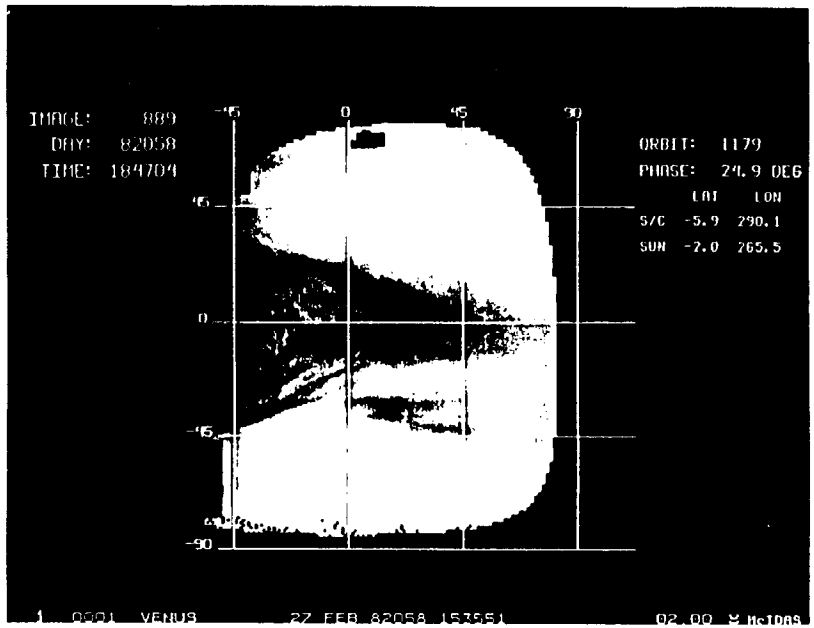

Figure 2a.

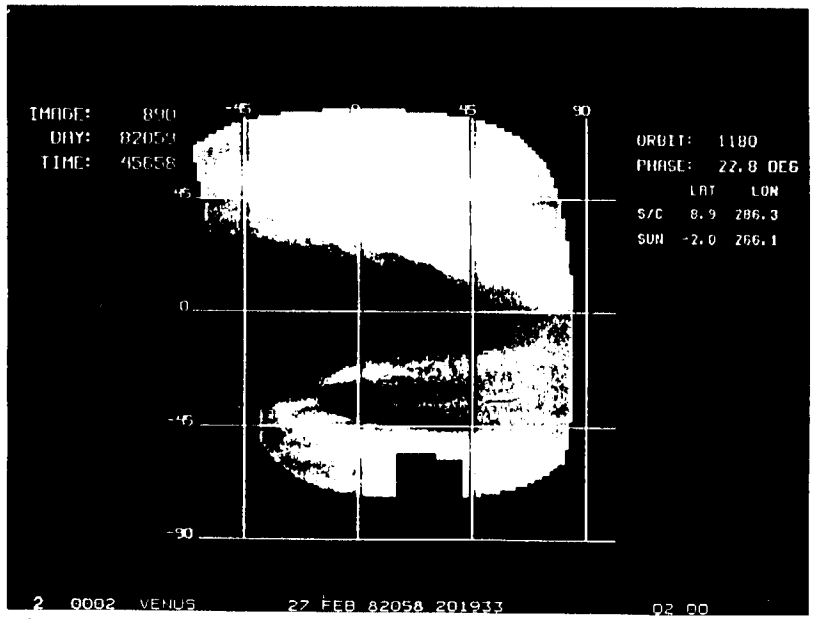

Figure 2b.

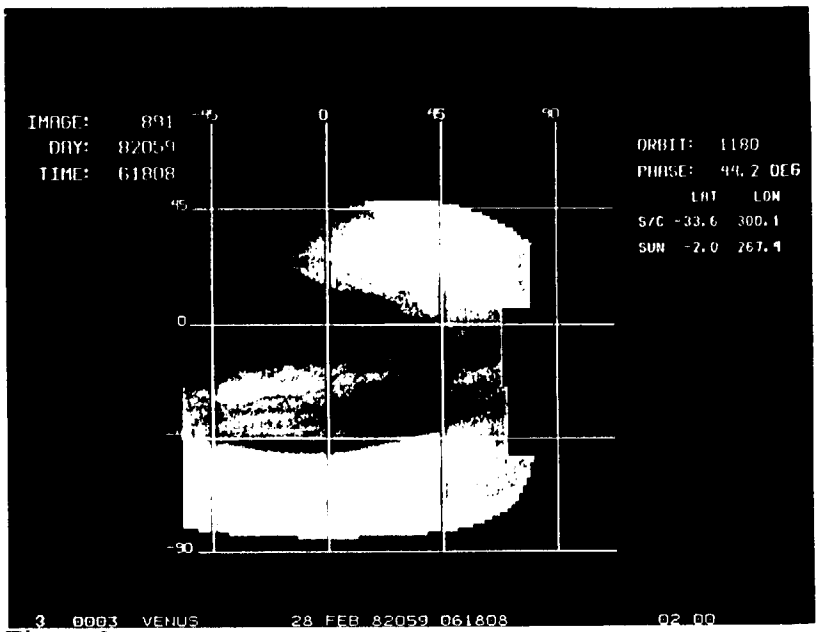

Figure 2c.

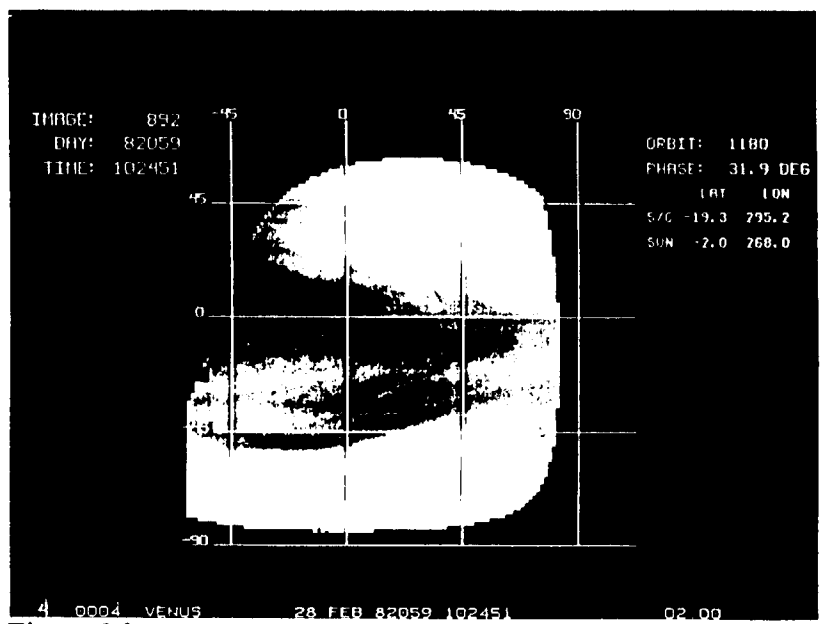

Figure 2d.

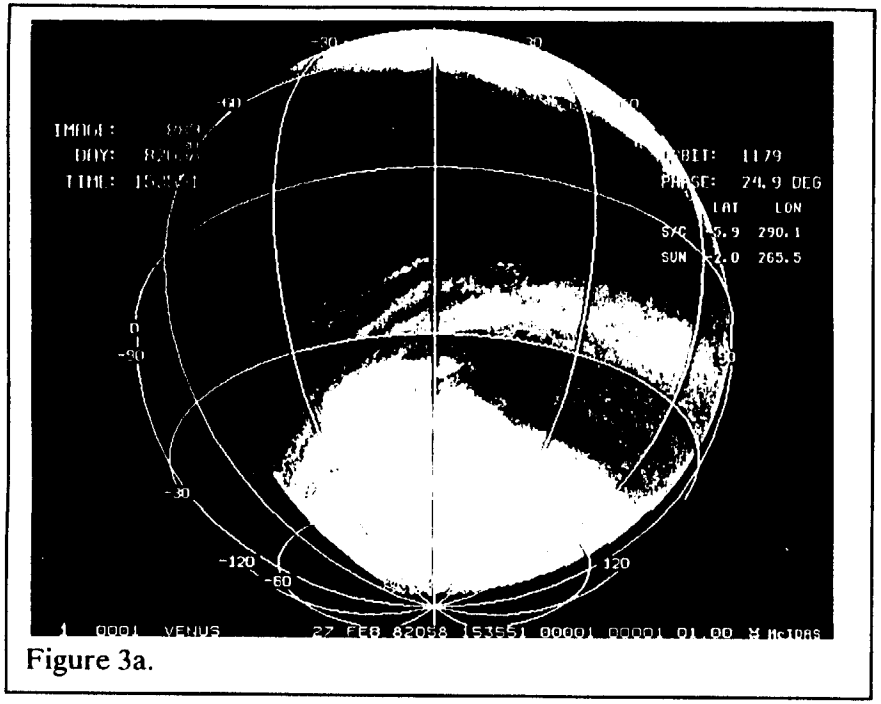

Figure 3a.

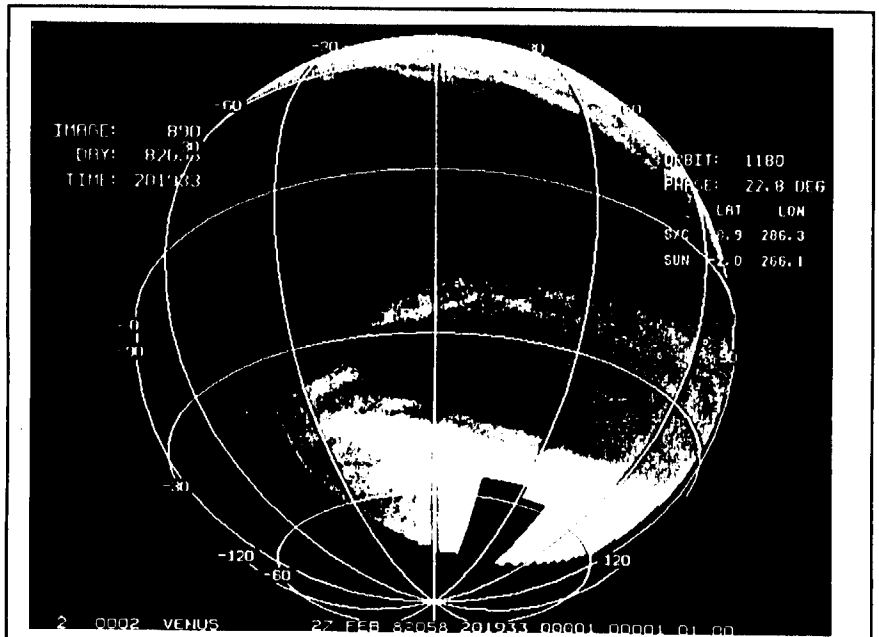

Figure 3b.

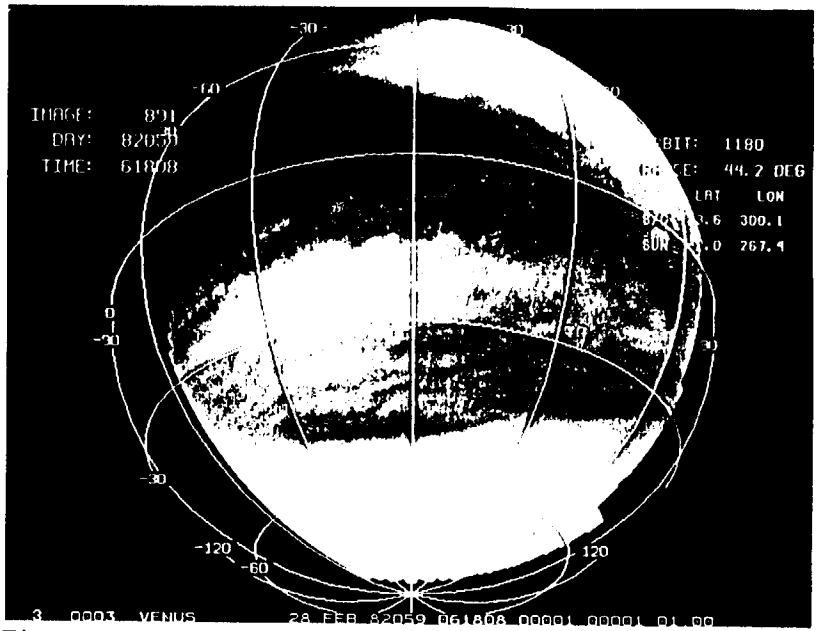

Figure 3c.

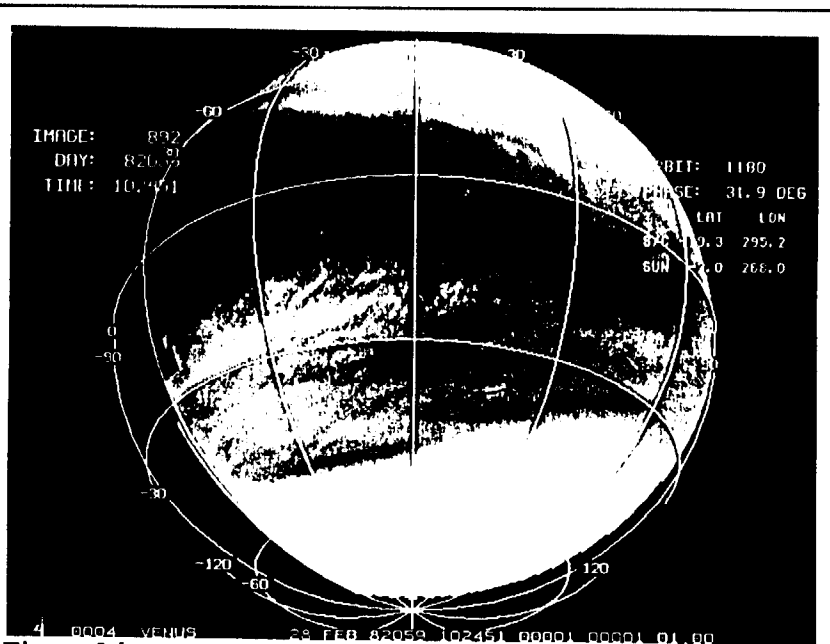

Figure 3d.

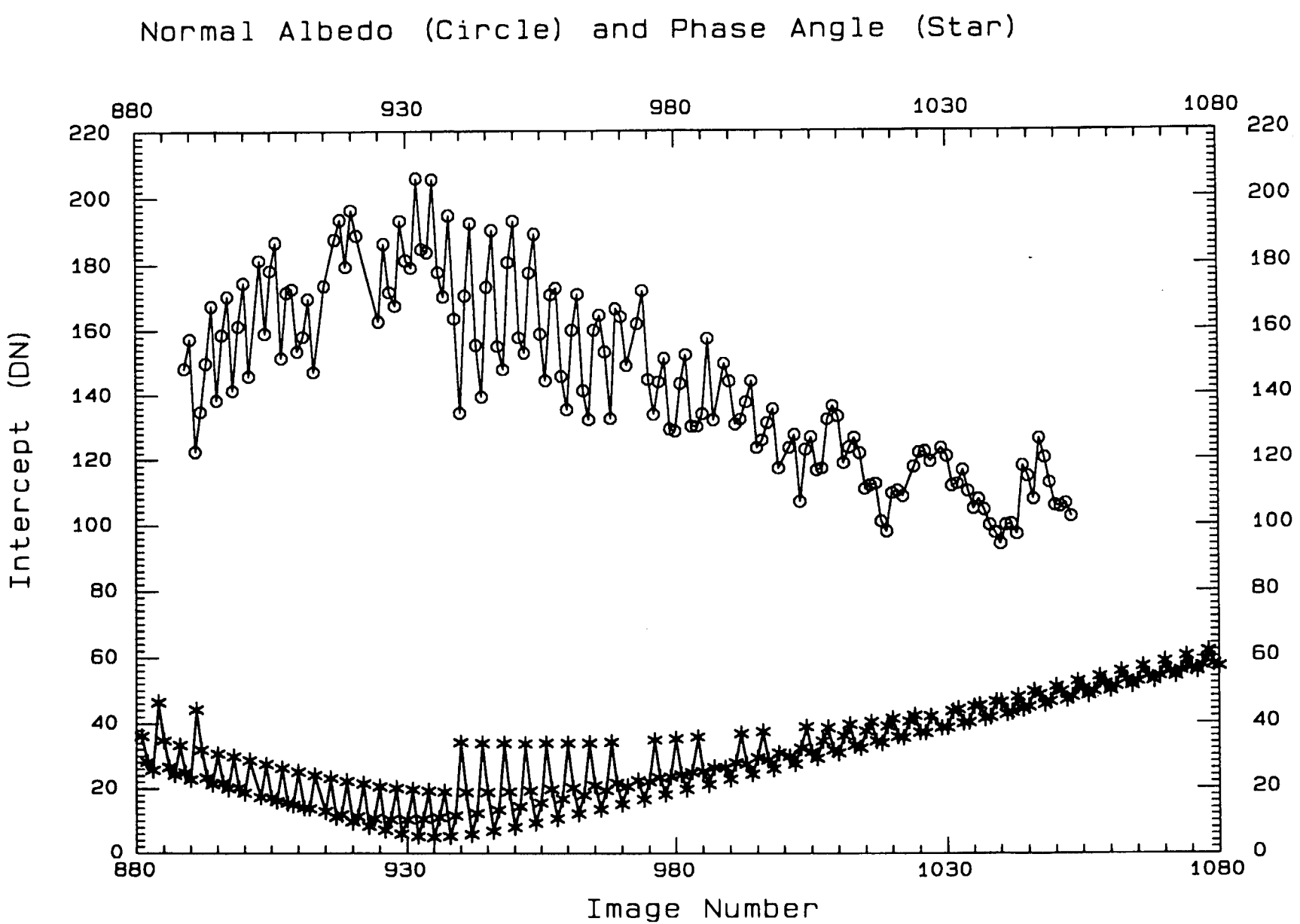
Normal Albedo (Circle) and Phase Angle (Star)
Intercept (DN)
Image Number
880
930
980
1030
1080
0
20
40
60
80
100
120
140
160
180
200
220

Figure 4a.

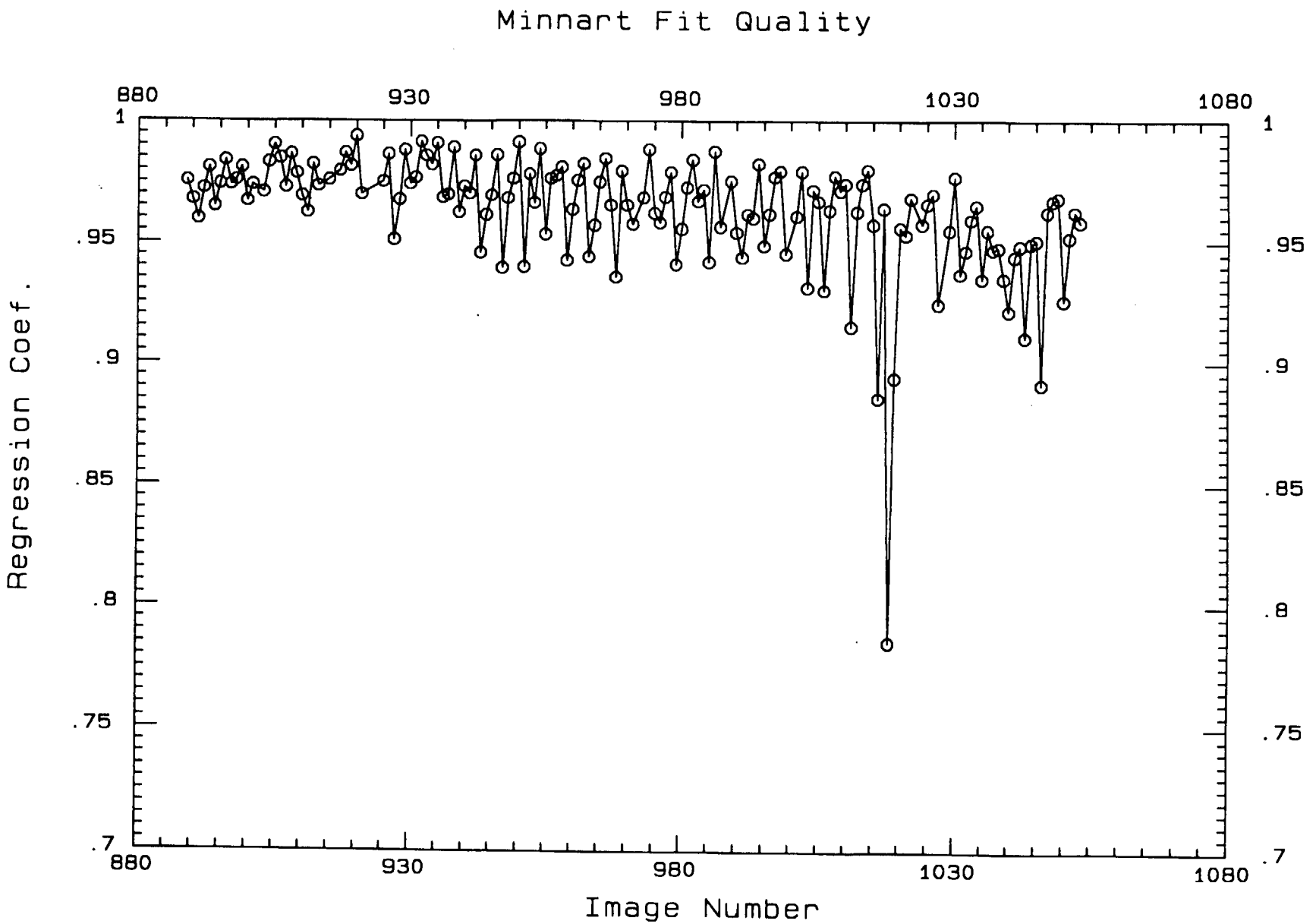
Minnart Fit Quality
880
930
980
1030
1080
1
.95
.9
.85
.8
.75
.7
Regression Coef.
Image Number

Figure 4c.

APPENDIX I

		Disk Center			Minnaert		
Image	Orbit	YYDDD	HHMMSS	Phase	Slope	Intcpt	R
889	1179	82058	153551	24.9	0.7565	148.2	0.9754
890	1180	82058	201933	22.8	0.7856	157.3	0.9676
891	1180	82059	61808	44.2	0.8417	122.5	0.9595
892	1180	82059	102451	31.9	0.8110	134.9	0.9722
893	1180	82059	153606	23.3	0.7576	149.9	0.9810
894	1181	82059	201954	21.3	0.8356	167.5	0.9647
895	1181	82060	102526	30.6	0.8099	138.4	0.9741
896	1181	82060	153638	21.7	0.7838	158.7	0.9838
897	1182	82060	201941	19.9	0.8274	170.5	0.9738
898	1182	82061	101350	29.8	0.8190	141.4	0.9758
899	1182	82061	153205	20.2	0.7747	161.3	0.9809
900	1183	82061	202210	18.6	0.8342	174.5	0.9670
901	1183	82062	101411	28.6	0.8159	145.9	0.9738
903	1184	82062	202216	17.3	0.8338	181.4	0.9707
904	1184	82063	101411	27.4	0.8479	159.1	0.9831
905	1184	82063	153147	17.1	0.7897	178.3	0.9904
906	1185	82063	202153	16.1	0.8152	186.7	0.9847
907	1185	82064	101425	26.2	0.8019	151.5	0.9727
908	1185	82064	153142	15.5	0.7666	171.6	0.9864
909	1186	82064	202143	14.9	0.7716	172.7	0.9784
910	1186	82065	101508	25.1	0.8562	153.6	0.9691
911	1186	82065	153126	14.0	0.7053	158.1	0.9623
912	1187	82065	202125	13.8	0.7641	169.7	0.9821
913	1187	82066	101426	24.1	0.7921	147.2	0.9732
915	1188	82066	202108	12.8	0.7627	173.7	0.9757
917	1188	82067	153050	11.1	0.7828	187.7	0.9794
918	1189	82067	202052	11.9	0.8081	193.5	0.9868
919	1189	82068	101410	22.2	0.8661	179.5	0.9815
920	1189	82068	153013	9.6	0.7927	196.4	0.9937
921	1190	82068	202014	11.2	0.7895	188.9	0.9698
925	1191	82070	101409	20.6	0.8201	162.8	0.9750
926	1191	82070	152916	7.1	0.7805	186.3	0.9863
927	1191	82070	201917	10.4	0.7506	171.7	0.9510
928	1193	82071	101243	20.1	0.8270	167.6	0.9675
929	1193	82071	152827	6.0	0.7783	193.1	0.9879
930	1193	82071	201821	10.3	0.7548	181.3	0.9740
931	1194	82072	101219	19.6	0.8479	179.1	0.9766
932	1194	82072	152754	5.3	0.8040	205.9	0.9914
933	1194	82072	201801	10.5	0.7508	184.6	0.9856
934	1195	82073	101144	19.2	0.8538	183.6	0.9819
935	1195	82073	152706	5.0	0.7930	205.5	0.9909
936	1195	82073	201717	10.9	0.7282	177.7	0.9684
937	1195	82074	101109	18.9	0.8125	170.2	0.9696
938	1195	82074	152619	5.2	0.7760	194.6	0.9891
939	1196	82074	201646	11.5	0.6879	163.6	0.9623
940	1196	82075	60730	34.0	0.8530	134.4	0.9730
941	1196	82075	101111	18.8	0.8268	170.6	0.9701
942	1196	82075	152533	5.8	0.7768	192.4	0.9858
943	1197	82075	201626	12.3	0.6587	155.5	0.9458

944	1197	82076	60727	33.8	0.8754	139.5	0.9613
945	1197	82076	101036	18.8	0.8348	173.3	0.9694
946	1197	82076	152447	6.8	0.7697	190.3	0.9860
947	1198	82076	201605	13.3	0.6563	155.1	0.9395
948	1198	82077	60715	33.7	0.9031	147.9	0.9682
949	1198	82077	101001	18.9	0.8516	180.7	0.9762
950	1198	82077	152345	8.0	0.7739	193.0	0.9911
951	1199	82077	201521	14.3	0.6625	157.8	0.9398
952	1199	82078	60700	33.6	0.9155	153.0	0.9780
953	1199	82078	100925	19.2	0.8297	177.5	0.9662
954	1199	82078	152258	9.3	0.7668	189.1	0.9883
955	1200	82078	201434	15.5	0.6727	158.8	0.9533
956	1200	82079	60645	33.7	0.8816	144.4	0.9762
957	1200	82079	100914	19.6	0.8149	170.8	0.9774
958	1200	82079	152209	10.6	0.7252	172.8	0.9810
959	1201	82079	201412	16.7	0.6291	145.8	0.9426
960	1201	82080	60640	33.7	0.8818	135.4	0.9635
961	1201	82080	100758	20.1	0.7915	160.0	0.9755
962	1201	82080	152119	12.1	0.7631	171.0	0.9824
963	1202	82080	201327	17.9	0.6401	141.3	0.9441
964	1202	82081	60646	33.8	0.8514	132.3	0.9571
965	1202	82081	100719	20.8	0.7977	160.0	0.9749
966	1202	82081	152012	13.5	0.7227	164.5	0.9846
967	1203	82081	201301	19.3	0.6916	153.2	0.9654
968	1203	82082	60638	34.1	0.7804	132.6	0.9357
969	1203	82082	100638	21.5	0.8023	166.5	0.9796
970	1203	82082	151932	15.0	0.7083	164.0	0.9654
971	1204	82082	201147	20.6	0.6558	149.0	0.9576
973	1204	82083	100529	22.3	0.7881	161.9	0.9685
974	1204	82083	151834	16.5	0.7703	172.0	0.9883
975	1205	82083	201139	22.0	0.6692	144.7	0.9620
976	1205	82084	60541	34.7	0.8595	133.9	0.9581
977	1205	82084	100517	23.2	0.7467	143.9	0.9687
978	1205	82084	151745	18.1	0.7138	151.2	0.9790
979	1206	82084	201032	23.4	0.6275	129.3	0.9410
980	1206	82085	60546	35.1	0.8536	128.7	0.9556
981	1206	82085	100437	24.1	0.7707	143.4	0.9727
982	1206	82085	151639	19.6	0.7368	152.3	0.9841
983	1207	82085	201030	24.8	0.6491	130.2	0.9670
984	1207	82086	60503	35.6	0.8410	130.1	0.9717
985	1207	82086	100406	25.1	0.6973	134.0	0.9421
986	1207	82086	151555	21.1	0.7658	157.4	0.9875
987	1208	82086	200939	26.3	0.6518	132.1	0.9565
989	1208	82087	100318	26.2	0.7922	149.6	0.9753
990	1208	82087	151454	22.7	0.6863	144.1	0.9542
991	1209	82087	200844	27.7	0.6457	130.8	0.9440
992	1209	82088	60434	36.7	0.8306	132.3	0.9616
993	1209	82088	100238	27.3	0.7478	137.6	0.9601
994	1209	82088	151402	24.2	0.7345	144.2	0.9824
995	1210	82088	200746	29.2	0.6375	123.5	0.9487
996	1210	82089	60413	37.3	0.8179	125.9	0.9617
997	1210	82089	100130	28.5	0.7474	131.2	0.9770
998	1210	82089	151304	25.8	0.7281	135.5	0.9794
999	1211	82089	200707	30.6	0.6425	117.2	0.9454

1001	1211	82090	100042	29.6	0.7453	123.5	0.9608
1002	1211	82090	151215	27.3	0.7203	127.5	0.9793
1003	1212	82090	200659	32.2	0.5873	107.0	0.9314
1004	1212	82091	60329	38.7	0.8270	123.0	0.9716
1005	1212	82091	100026	30.9	0.7585	126.8	0.9670
1006	1212	82091	154541	29.1	0.6076	116.7	0.9303
1007	1213	82091	202812	34.4	0.6617	117.2	0.9633
1008	1213	82092	62154	38.5	0.8378	132.3	0.9774
1009	1213	82092	103145	31.6	0.7815	136.4	0.9713
1010	1213	82092	154537	30.6	0.7222	133.2	0.9741
1011	1214	82092	202733	35.9	0.6222	118.8	0.9152
1012	1214	82093	62139	39.4	0.8046	123.5	0.9627
1013	1214	82093	103108	33.0	0.7664	126.6	0.9741
1014	1214	82093	154447	32.2	0.7204	121.8	0.9800
1015	1215	82093	202701	37.4	0.6579	110.8	0.9574
1016	1215	82094	62143	40.2	0.9607	111.9	0.8856
1017	1215	82094	103026	34.3	0.7382	112.5	0.9640
1018	1215	82094	152700	33.7	0.6978	101.0	0.7853
1019	1216	82094	202624	38.9	0.5856	97.9	0.8939
1020	1216	82095	62056	41.2	0.7877	109.5	0.9561
1021	1216	82095	102951	35.7	0.7332	110.4	0.9532
1022	1216	82095	154346	35.4	0.6925	108.6	0.9683
1024	1217	82096	62016	42.1	0.8084	117.7	0.9577
1025	1217	82096	102834	37.0	0.7655	122.0	0.9659
1026	1217	82096	154154	36.9	0.7271	122.4	0.9700
1027	1218	82096	202503	41.9	0.6882	119.3	0.9246
1029	1218	82097	102731	38.4	0.7528	123.4	0.9550
1030	1218	82097	154103	38.5	0.7243	120.9	0.9769
1031	1219	82097	202418	43.4	0.6572	111.8	0.9371
1032	1219	82098	61913	44.1	0.7549	112.4	0.9467
1033	1219	82098	102707	39.8	0.7596	116.7	0.9594
1034	1219	82098	154013	40.1	0.7003	110.2	0.9651
1035	1220	82098	202345	44.9	0.6462	104.8	0.9351
1036	1220	82099	61912	45.2	0.7797	107.7	0.9550
1037	1220	82099	102619	41.2	0.7155	104.5	0.9471
1038	1220	82099	153842	41.7	0.6651	99.8	0.9479
1039	1221	82099	202301	46.4	0.6378	97.6	0.9352
1040	1221	82100	61847	46.2	0.7015	94.3	0.9216
1041	1221	82100	102530	42.6	0.7173	99.9	0.9442
1042	1221	82100	153818	43.2	0.6862	100.1	0.9486
1043	1222	82100	202226	47.9	0.6106	97.2	0.9108
1044	1222	82101	102403	44.0	0.7722	118.0	0.9496
1045	1222	82101	153646	44.8	0.7151	114.8	0.9509
1046	1223	82101	202152	49.5	0.6215	107.7	0.8914
1047	1223	82102	61745	48.4	0.8438	126.4	0.9625
1048	1223	82102	102351	45.5	0.7817	120.4	0.9671
1049	1223	82102	153543	46.4	0.7235	112.8	0.9683
1050	1224	82102	202042	51.0	0.6558	105.8	0.9260
1051	1224	82103	61653	49.5	0.7670	105.5	0.9521
1052	1224	82103	102300	46.9	0.7519	106.4	0.9626
1053	1224	82103	153520	47.9	0.7043	102.5	0.9584